^{1}H and ^{2}H NMR of Hydrogen Adsorption on Carbon Nanotubes

Kai Shen and Tanja Pietrass*

Department of Chemistry, New Mexico Tech, Socorro, New Mexico 87801

Received: December 17, 2003; In Final Form: May 11, 2004

Hydrogen adsorption on carbon nanotubes was studied with ^{1}H and ^{2}H NMR spectroscopy. A total of eight single- and multiwalled carbon nanotube samples provided by various manufacturers and synthesized by different production methods were investigated before and after an oxidative purification procedure. NMR data are corroborated by TEM, ICP-MS, and ESR spectroscopy. The presence of residual metal catalyst particles causes considerable broadening of the spectra. While susceptibility broadening and dipolar interactions often dominate the ^{1}H NMR spectra, quadrupolar interactions lead to additional broadening in the ^{2}H NMR. Smaller line widths in the ^{2}H NMR data allowed for free hydrogen gas and adsorbed hydrogen to be distinguished. The adsorption is fast and reversible and must be described as physisorption. Hydrogen uptake capacities at a pressure of 1480 kPa and at ambient temperature were estimated to be about 0.1 wt %.

1. Introduction

Iijima's discovery of carbon nanotubes (CNT's) in 1991 sparked intense research activity due to their unusual mechanical and electronic properties.[1] Dillon et al.[2] suggested in 1997 that CNT's may provide hydrogen storage capacities exceeding those of any other known material, and also exceeding the benchmark set by the Department of Energy for an economically viable hydrogen storage material (6.5% storage capacity by weight, wt %).[3] To date, the reported storage capacities from experimental and theoretical results vary from less than 1 wt % to about 14 wt %.[4−8] The ensuing controversy about CNT's hydrogen uptake capacity[4,9] and sorption mechanism[10−15] has not been settled yet. This is probably related to the fact that a large number of production and purification methods exist, and hence every researcher is effectively studying a different system. We are trying to address this issue by investigating a large number of commercially available single- and multiwalled carbon nanotubes using NMR spectroscopy. Samples were studied before and after purification, and carefully characterized by transmission electron microscopy (TEM) and inductively coupled plasma analysis/mass spectrometry (ICP-MS) as described previously.[16] Using NMR spectroscopy of the two hydrogen isotopes ^{1}H and ^{2}H with nuclear spin $I = {}^1/_2$ and 1, respectively, we obtain complementary information that allows us to distinguish dipolar, chemical shift, and quadrupolar contributions.

2. Experimental Section

Characteristics of our samples as provided by the manufacturers together with our ICP-MS (Agilent 7400) data before and after purification are presented in Table 1.[16] In the following, the samples will be referred to as MRGC, MRMWC, MRSW, and CNI, as introduced in Table 1. All samples were purified with use of an oxidative procedure.[17] MRGC, MRMWC, and MRSW were purchased from Mer Corporation (Tucson, AZ), and CNI from Carbon Nanotechnologies (Houston, TX). The samples were further characterized before and after purification with TEM (JEOL JEM 2010). In addition, three other multiwalled carbon nanotube samples provided by Nanolab (Newton, MA), and one single-walled sample from Carbolex (Lexington, KY), were investigated. Although TEM micrographs clearly show the presence of nanotubes and only a small amount of impurities in the Nanolab samples, neither ESR nor NMR signals could be obtained.[16] The quality of the Carbolex sample was questionable. ICP-MS data revealed an impossibly high metal content, and only a ferromagnetic resonance was detected with ESR,[16] in agreement with the results by Chen et al.[18] As expected, ^{1}H NMR spectra after hydrogen exposure yielded broad, undefined signals with poor signal-to-noise ratio. TEM micrographs revealed a very low content of carbon nanotubes. The CNT's are embedded in carbon-coated metal particles. Hence, Nanolab and Carbolex data will not be discussed further.

Samples were weighed and loaded into 5-mm Pyrex tubes which were connected to a vacuum rack and either a hydrogen (Matheson Trigas, UHP) or deuterium (D_2 99.6%, Cambridge Isotope Laboratories) gas cylinder. Gas pressures ranged from 101 to 1480 kPa. Prior to gas exposure, the samples were heated under vacuum (1 Pa) to 853 K for 2 h to remove impurities such as water and adsorbed gases. Heating also aids in the removal of functional groups at the tips of the nanotubes or at defects sites generated during the purification procedure.[19] NMR spectra were acquired with a Bruker MSL-400/Apollo Tecmag spectrometer at a Larmor frequency of 400.127 MHz for ^{1}H and 61.423 MHz for ^{2}H. Chemical shifts and line widths at 1480 kPa hydrogen pressure are summarized in Table 2 for all samples.

3. Results and Discussion

Hydrogen exists in two forms, *o*-H_2, where the protons are in a triplet state, and *p*-H_2, with the protons in a singlet state. Interconversion of the two in the absence of a catalyst is slow. Only *o*-H_2 contributes to the NMR signal. Relaxation occurs through intermolecular dipolar couplings and spin rotation.[20] In our apparatus, we measured a chemical shift for pure hydrogen gas of 6.8 ppm regardless of pressure. The isotope shift between $^1H_2$ and $^2H_2$ is very small, only 0.078 ppm at 300 K.[21]

3.1. Multiwalled Carbon Nanotubes. *3.1.1. MRGC.* The multiwalled samples, MRMWC and MRGC, were synthesized

* Address correspondence to this author.

10.1021/jp037909z CCC: $27.50
Published on Web 06/19/2004

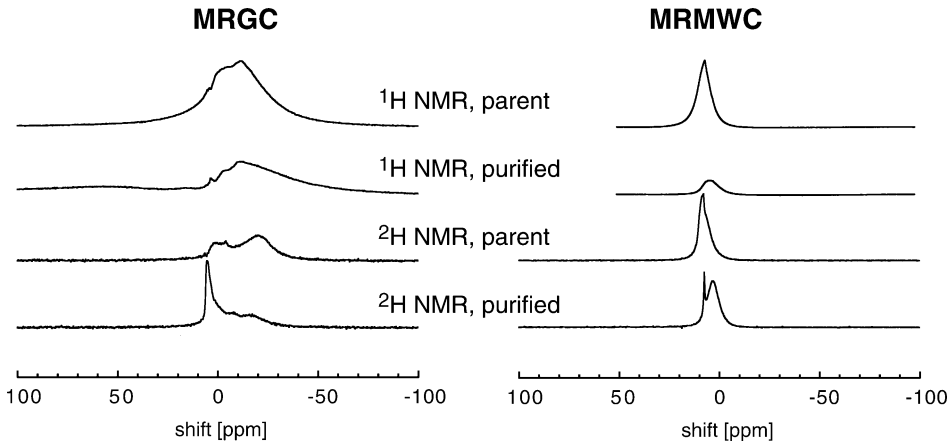

Figure 1. ^{1}H and ^{2}H NMR of hydrogen-exposed multiwalled carbon nanotube samples at a hydrogen pressure of 1480 kPa. The small signal component at about 4 ppm in the ^{1}H NMR spectra is due to the NMR probe background.

TABLE 1: Sample Characteristics[a]

sample	prod method	structure	length [μm]	diam [nm]	purity [%]	metal impurities	ICP-MS [wt %]	ICP-MS pur [wt %]
MRGC	CAD	multiwalled, closed	N/A	50	N/A	none	1	0.3
MRMWC	CVD	multiwalled, closed	50	N/A	>95	Fe < 0.1%	4	3
MRSW	CAD	single-walled, open	up to 100	1.3	>90	Co, Ni	32	15
CNI	HiPCO	single-walled[b]	0.1−1	1	<72	Fe 25%	N/A	20

[a] All entries except the ICP-MS data are as provided by the manufacturer. CAD = carbon arc discharge, CVD = chemical vapor deposition, HiPCO = high pressure injection of carbon monoxide. ICP-MS data are given in gmetal/graw material; ICP-MS pur = ICP-MS results after purification. [b] The manufacturer did not provide information about tube ends

TABLE 2: ^{1}H and ^{2}H NMR Shifts (δ), Line Widths ($\Delta\nu$), and Ratio r ($=\Delta\nu(^1\text{H})/\Delta\nu(^2\text{H})$) at a Hydrogen/Deuterium Pressure of 1480 kPa[a]

sample	$\delta(^1\text{H})$ [ppm]	$\Delta\nu(^1\text{H})$ [kHz]	$\delta(^2\text{H})$ [ppm]	$\Delta\nu(^2\text{H})$ [kHz]	r
MRGC	−11, −2	12.7	−20, −2	1.93	∼6.6
MRGC pur	−11, −2	17.2	5	0.35	∼49
MRMWC	7.5	2.72	7.9	0.34	∼8
MRMWC pur	5	3.74	3.0	0.39	∼9.6
MRSW	16	16.1	15	0.83	∼19
MRSW pur	5.6	2.40	2.5	0.15	∼16
CNI	10	13.5	N/A	N/A	N/A
CNI pur	8.9	2.42	8	0.26	∼9.3

[a] Errors in chemical shifts are estimated to ±1 ppm for integer values, and to ±0.5 ppm for values reported to one decimal place.

with chemical vapor deposition and carbon arc discharge, respectively. MRGC was made without a metal catalyst. The ^{1}H NMR spectra of hydrogen-exposed MRGC show a broad signal centered at −11 ppm. With increasing hydrogen pressure, another signal component emerges at −2 ppm, and the overall line width increases to 12.7 kHz at 1480 kPa (Figure 1). ESR data reveal the superposition of two lines, one assigned to graphitic particles, and the other to conducting nanotubes.[16] TEM pictures give evidence of nano-onion-like structures which are not removed upon purification (Figure 2). However, both ESR and ^{1}H NMR spectra show significant changes after purification. While the ESR resonance assigned to graphitic particles disappears, the ^{1}H NMR spectra have a lower signal-to-noise ratio than those for the parent material. The ^{1}H NMR resonance at −2 ppm is diminished in intensity when compared to the component at −11 ppm (Figure 1). The line width of the peak component at −11 ppm is pressure dependent and increases from 4.4 kHz at 101 kPa to 17.2 kHz at 1480 kPa. The large deviation from the typical chemical shift range of hydrogen (0−12 ppm) might be a Knight shift caused by the interaction of hydrogen with metallic nanotubes. The presence of graphitic particles, nanotubes, and nano-onions revealed by TEM suggests

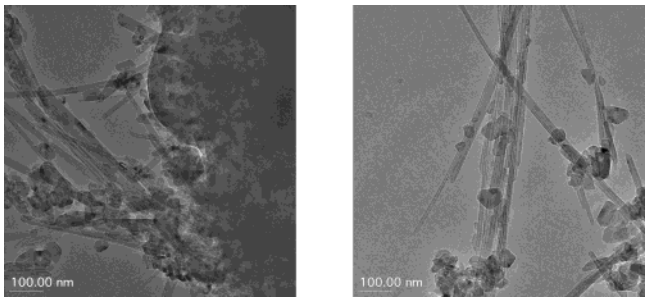

Figure 2. TEM micrographs of MRGC before (left) and after (right) purification.

the assignment of the two ^{1}H NMR resonances to hydrogen interacting with these structures. On the basis of the ESR and TEM data, the ^{1}H NMR signal component at −2 ppm can hence be assigned to hydrogen on graphitic particles.[16] The preferential occupation of the site giving rise to the signal component at −11 ppm thus suggests that nanotubes and onions present stronger adsorption sites for hydrogen than graphitic particles.

Evacuation of the sample led to the immediate and complete disappearance of the ^{1}H signal. The same effect was observed for all other samples, indicating that the adsorption process is physical in nature, fast, and reversible, in agreement with the results by Smith et al.[22]

The signal for free hydrogen gas was only observable when lowering the sample in the receiver coil to a position where the sample tube region filled with nanotubes was immersed in the receiver coil one-sixth of the way. The remaining volume above the sample thus gave rise to the resonance of the pure gas phase. Free gas in the interparticle space was unobservable, most likely caused by susceptibility broadening of the resonance due to contact with conducting particles. Similarly, Schmid et al. were able to observe the gas resonance only at temperatures below 35 K.[23]

To explore the exchange dynamics between the gas phase and the adsorbed phase, two-dimensional ^{1}H NMR exchange

experiments[24] were carried out on the partially inserted, unpurified sample. The dynamics were probed on a time scale from $\tau = 5$ μs to 5 ms at a gas pressure of 446 kPa. It should be noted that the spin−lattice relaxation time T_1 of hydrogen in contact with this sample is about 5 ms, so that for the longest exchange times τ, relaxation is affecting the overall signal intensity. No cross-peaks were observed for any value of τ, indicating that the exchange of the two phases must be slower than 5 ms at this pressure. When integrating the peak areas and fitting them to an exponential decay as a function of τ, a more rapid decay was observed for the gas phase (0.15 ms) than for the adsorbed phase (0.39 ms). Both of these time constants are shorter than T_1 (4.8 ms at 170 kPa), and are also shorter than T_1 for the free gas (1.5 ms at 1500 kPa),[25] in agreement with the results by Yu[26] and Kleinhammes,[27] who studied methane and ethane adsorption.

^{2}H NMR data mostly confirm the results from ^{1}H NMR (Figure 1). The most striking difference is that the signal-to-noise ratio is higher for purified MRGC. Furthermore, *chemical* shifts should be equal on a ppm scale for both isotopes. However, in the unpurified sample, two main ^{2}H NMR signal components centered around −20 and −2 ppm (at 1480 kPa) are observed. These two components are better separated than in the ^{1}H NMR. While the component at −2 ppm occurs in both spectra, the other one, tentatively assigned to hydrogen interacting with metallic nanotubes, gives rise to a more negative shift in the ^{2}H NMR. The difference is not compatible with a Knight shift or chemical shift.

In addition, the shift observed for the purified MRGC sample differs for ^{1}H and ^{2}H NMR. While similar to the ^{1}H NMR results the upfield part of the resonance is reduced to an ill-defined tail, the downfield component occurs at about 5 ppm with increased intensity. The exact same sample was used for the ^{1}H and ^{2}H NMR experiments, so the difference in the spectra can only be due to the properties of the two nuclear isotopes. The narrower line width observed with ^{2}H NMR indicates a reduction in dipolar couplings or susceptibility broadening due to the much smaller γ of ^{2}H. The reduction factor is close to the ratio of the γ values of 6.5 as expected for susceptibility broadening. For dipolar broadening, a scaling factor of γ^2 would be expected.

3.1.2. MRMWC. The ^{1}H NMR spectra of the MRMWC parent sample show one clearly defined resonance in the pressure range from 101 kPa to 1480 kPa centered at 7.5 ppm (Figure 1). An increase in pressure causes a small increase in line width, from 2.0 kHz at 170 kPa to 2.7 kHz at 1480 kPa. Upon purification, the signal-to-noise ratio decreases and the line width increases while the line position is not affected. Overall, the signal-to-noise ratio is higher for MRMWC than for MRGC despite the slightly larger sample amount used (MRGC, 65.9 mg; MRMWC, 66.5 mg).

It has been shown that hydrogen uptake for multiwalled carbon nanotubes is proportional to their diameter and density of defect sites.[28] MRMWC has a wide distribution of diameters as shown by TEM, so the difference in signal intensity cannot be related to diameter. Lower graphitization of the walls in the MRMWC sample leads to a higher density of defects, and can thus explain the higher ^{1}H NMR signal intensity.

TEM micrographs reveal further important features. First, the MRMWC parent sample contains a significant number of carbon nanofibers, and second, the nanotubes, as well as the nanofibers, are severely damaged upon purification (Figure 3). Structural damage to the tube walls is expected to cause the formation of defect sites. This is confirmed by ESR where a shift in *g*-factor as well as a change in line shape from Dysonian to symmetric is observed.[16] Moreover, on average, there seem to be less conduction electrons present in the MRMWC sample when compared to MRGC as evidenced by the absence of a Knight shift in the NMR spectra as well as a more symmetric line shape in the ESR. This leads to two possible conclusions: the carbon nanotubes in MRMWC are predominantly semiconducting, or hydrogen interacts more strongly with nonconducting carbon nanofibers. The increase in line width with pressure is most likely caused by stronger intermolecular homonuclear dipolar couplings due to the increasing spin density.

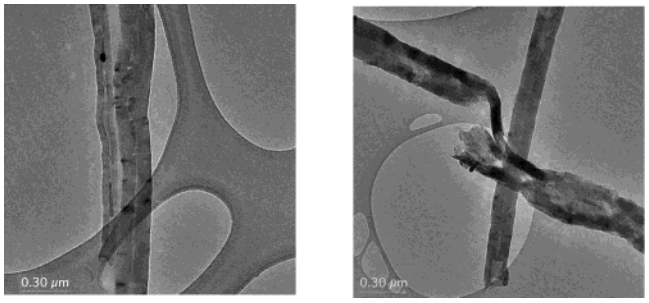

Figure 3. TEM micrographs of MRMWC before (left) and after (right) purification.

Due to the possible introduction of additional quadrupolar interactions upon usage of ^{2}H, the comparison of the line widths of the two hydrogen isotopes is not sufficient evidence to identify the dominant contribution to the line width. Since the dipolar coupling constants for the two isotopes scale with the square of their respective γ values, a ratio of 42 would be expected for the line widths of the two isotopes. The experimental ratio is ∼8 for the unpurified sample, which is much closer to the ratio of the γ values. Hence, broadening seems to be mainly caused by the magnetic susceptibility with some contributions from dipolar interactions. The smaller line width for ^{2}H allows for the distinction between hydrogen in the free gas and in the adsorbed phase. In the ^{2}H NMR spectra of the parent material at a pressure of 1480 kPa, a narrow resonance at 7 ppm can barely be distinguished from the broad resonance centered at 7.9 ppm (Figure 1). Purification causes this resonance to shift to 3 ppm as well as an increase in line width from 340 to 390 Hz. The gas resonance is clearly visible at 7 ppm after purification. The ratio of the line widths of the parent to the purified samples is about 1.4 for ^{1}H NMR and about 1.2 for ^{2}H NMR. This similarity suggests that the larger line width in the purified material is due to dipolar couplings between hydrogen nuclear spins and unpaired electronic spins from defect sites. This is consistent with the fact that the line width of the broader peak component in the ^{2}H NMR spectra decreases slightly with pressure, while the component for the gas-phase resonance remains constant (Figure 1). With increasing pressure, defect sites become saturated with hydrogen, thus mitigating the nuclear−electronic couplings. In the gas phase, however, the homonuclear dipolar interactions increase due to a higher spin density.

3.2. Single-Walled Carbon Nanotubes. Single-walled carbon nanotubes prepared by different techniques were purchased from three manufacturers. MRSW was synthesized by using carbon arc discharge with a Ni/Y and a Co/Ni bimetallic catalyst, respectively. CNI was produced by using the HiPCO process (high-pressure injection of carbon monoxide) with Fe as catalyst.

3.2.1. MRSW. TEM, ICP-MS, and ESR data showed that the MRSW sample was high quality and contained a significant fraction of nanotubes. A ferromagnetic resonance was detected

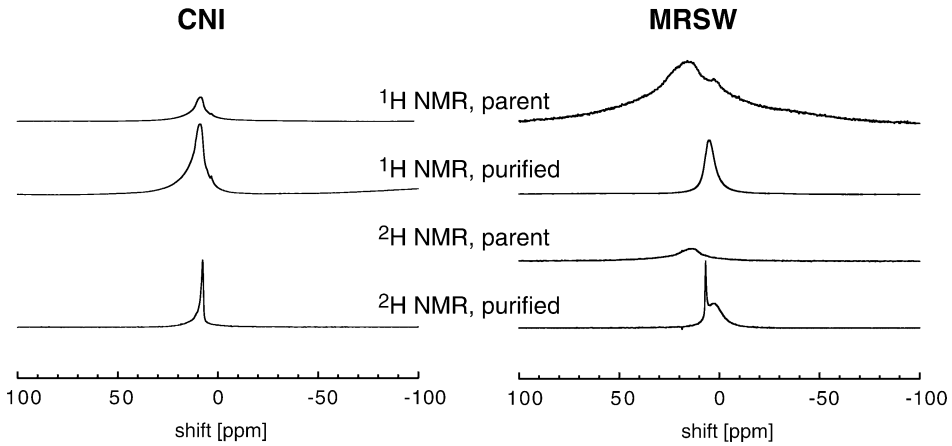

Figure 4. ^{1}H and ^{2}H NMR of hydrogen-exposed single-walled carbon nanotube samples at a hydrogen pressure of 1480 kPa.

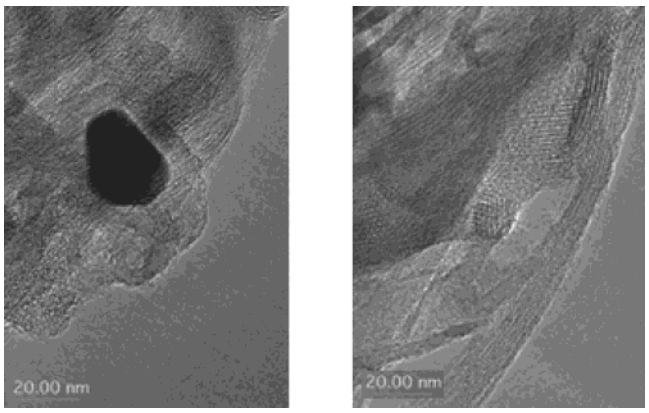

Figure 5. TEM micrographs of MRSW before (left) and after (right) purification.

with ESR before purification,[16] consistent with a metal content of 32 wt % found by ICP-MS (Table 1). The ^{1}H NMR spectra of this sample after hydrogen exposure revealed a broad resonance with poor signal-to-noise ratio as expected in the presence of conducting particles (Figure 4). In addition, the amount of sample was considerably smaller than that for MRGC and MRMWC (17.8 mg). The ^{1}H NMR resonance seems to be composed of several components, with the one at 14 ppm becoming dominant as hydrogen pressure increases. The overall line width is about 16.1 kHz at a pressure of 1480 kPa. At lower pressures, the resonance covers approximately 30 kHz.

As shown by TEM (Figure 5), purification causes a dramatic improvement in ^{1}H NMR signal-to-noise ratio based on the removal of metallic particles. Only one resonance is visible, which shifts slightly downfield with increasing pressure (from 3 ppm at 136 kPa to 5.6 ppm at 1480 kPa). At a hydrogen pressure of 1480 kPa, the line width is 2.4 kHz, which is significantly narrower than that before purification. When lowering the sample out of the center of the NMR pick-up coil, a large, narrow peak emerges at 6.8 ppm, the chemical shift of pure hydrogen gas. Calculations suggest that physisorbed hydrogen prefers to reside outside the interior of single-walled carbon nanotubes, and the increase in signal intensity is thus not expected to arise from hydrogen in the interior.[29] Kleinhammes et al.[27] also report, using NMR, that molecular hydrogen cannot enter the insterstitial sites of SWNT bundles. Calculations for gas adsorption on a nonhomogeneous bundle of CNT's, however, showed that gases readily adsorb in the interstitial channels, while this is not the case for homogeneous bundles.[30]

^{2}H NMR results largely confirm the ^{1}H NMR findings. While the spectra for the unpurified sample are noisy and reveal a broad, unstructured resonance centered at about 15 ppm and a line width of 830 Hz, the signal-to-noise ratio dramatically improves for the purified sample. Even at the lowest pressures, a resonance at 7 ppm assigned to the free gas can be distinguished. The broader resonance shifts from 1 ppm at 101 kPa of pressure to 2.5 ppm at 1480 kPa. The difference in peak position for the two isotopes indicates that the shift cannot be characterized as a *chemical* shift. The ratio of the line widths for the two isotopes at the highest pressure is about 20, implying that the line width cannot be solely determined by susceptibility broadening with possible contributions from dipolar and quadrupolar interactions. Furthermore, spectral hole burning and two-dimensional exchange experiments show that the line width is determined by a site heterogeneity and that mobility among different adsorption sites is diffusion limited.[31]

3.2.2. CNI. The last of the single-walled carbon nanotube samples, CNI, also gave rise to a ferromagnetic resonance in the ESR due to the large metal content. Accordingly, the ^{1}H NMR spectra reveal a resonance with low signal-to-noise ratio (Figure 4). After purification, a peak at 8.9 ppm with a line width of 2.4 kHz is observed. The ESR spectrum of the purified sample consists of a single, symmetric line indicative of defect sites.[16] Due to the low signal intensity in the ^{1}H NMR spectra, no ^{2}H NMR data were collected for the unpurified CNI sample.

Shiraishi and Ata[32] observed a narrow peak for hydrogen-exposed, purified nanotubes also synthesized by the HiPCO process. The line width of about 1 ppm, shift of 5.1 ppm, and relaxation time of 100−200 ms suggest that this peak originates from water. The authors chemically treated the sample with SO_2, which should result in a change in line position for water which was, however, not observed.[32] Our data indicate much broader line widths and shorter relaxation times for physisorbed hydrogen, and a relaxation time on the order of a few milliseconds for the pure gas.

^{2}H NMR spectra for purified CNI upon hydrogen exposure reveal an asymmetric peak that is most likely caused by the superposition of a broad and a narrow peak component. The latter is positioned at 7.7 ppm, and the former appears as a downfield tail. The line width of the narrow component is 90 Hz, indicative of free gas. The line width of the broader component can be estimated at about 260 Hz, and the ratio of the line widths for the two isotopes thus amounts to a factor of about 9, indicating that quadrupolar components significantly contribute to the line width.

4. Summary

A comparison of the integrated signal intensities as a function of pressure for all samples is shown in Figure 6. A linear

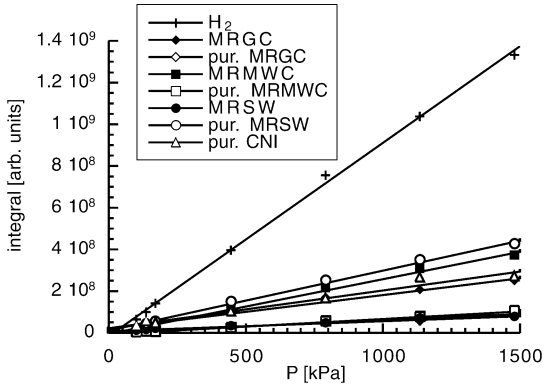

Figure 6. ^{1}H NMR integrated signal intensities as a function of pressure.

dependence is observed for all nanotube samples and also for pure hydrogen gas. Since the amount of sample used differed for the various types of nanotubes, the data cannot be compared on an absolute scale. The slopes of the lines, however, do not depend on the amount of sample. With increasing pressure, the spin density grows proportionally, and a linear dependence is expected for the free gas, as observed. Without strong adsorption occurring, the absolute values for the integrated signal intensities are expeceted to be smaller than those for the free gas due to the dead volume of the nanotubes.

Our data show that both the absolute value of the signal intensities and the slopes for any of the nanotube samples are smaller than those for the free gas. This is a clear indication that in the pressure range investigated and at ambient temperature the hydrogen uptake is not significant.

When using the integrated signal intensities for the pure gas to estimate the number of molecules represented by the signal observed for hydrogen in carbon nanotubes, a crude estimate of an upper limit in uptake capacity can be obtained.

Assuming that all the hydrogen is adsorbed, we can, from the volume of the pick-up coil and the signal intensity of the gas, calculate the mass of hydrogen corresponding to the observed signal on a CNT sample. For MRMWC, this amounts to 6.3×10^{-5} g for H_2 and 1.2×10^{-4} g for D_2. On the basis of a 66.5-mg sample, this translates into a hydrogen uptake capacity of about 0.1 wt % for H_2 and to about 0.2 wt % for D_2. For D_2, we can decompose the resonance into a component for the free gas, and one for adsorbed hydrogen. Their areas are roughly equal, yielding an uptake capacity of about 0.1 wt % for D_2.

Neither shifts nor line widths correlate with the production method, wall structure, or length and diameter of the tubes. NMR line positions are highly dependent on the presence of impurities. In general, a decrease in shift is observed upon purification, indicative of a reduced interaction with metallic particles.

5. Conclusions

Our data show that a combination of analytical techniques is necessary to give a picture of hydrogen adsorption on commercial carbon nanotube samples. Applying a single spectroscopic technique to a single sample may yield misleading data. The combination of sample characterization by using TEM and ICP-MS with spectroscopic techniques, here, ESR and NMR spectroscopy of the two hydrogen isotopes ^{1}H and ^{2}H, leads to the conclusion that none of the four different commercially available carbon nanotube samples presented high hydrogen storage capacities for pressures up to 1480 kPa and at ambient temperature. Susceptibility broadening and dipolar interactions among ^{1}H nuclei as well as possibly quadrupolar interactions of ^{2}H nuclei prevented the identification of distinct adsorption sites. Spectral hole-burning data and two-dimensional NMR exchange experiments gave some indication of the presence of heterogeneous adsorption sites. This in combination with theoretical results leads to the hypothesis that the preferred adsorption sites are the interstitial grooves in single-walled, bundled nanotubes.[30,31,33]

The data presented here clearly show that carbon nanotubes, as obtained from the manufacturers, are highly inhomogeneous systems. Interactions between hydrogen and the samples seem to originate in general from residual catalyst particles, graphitic particles, or other structures such as nano-onions. Purification simplified the spectra by removing paramagnetic and conducting particles. Only when pure carbon nanotubes were present that had retained their structural integrity could we study the interaction of the hydrogen gas with nanotubes.

Our data show no evidence of chemisorption. Defect sites were the preferred adsorption sites both in single- and multi-walled carbon nanotubes. Further studies at very low temperatures and low hydrogen pressures are planned to reduce the mobility of the hydrogen on the surface, and to minimize intermolecular interactions. Furthermore, the theoretically predicted ratios of velocities of the hydrogen isotopes inside the tubes are expected to change dramatically (up to 4 orders of magnitude depending on tube chirality) at temperatures below 100 K, which will be explored with NMR.[34]

Acknowledgment. This material is based upon work supported by the National Science Foundation under Grant No. 0107710.

References and Notes

(1) Iijima, S. *Nature* **1991**, *354*, 56−58.
(2) Dillon, A. C.; Jones, K. M.; Bekkedahl, T. A.; Kiang, C. H.; Bethune, D. S.; Heben, M. J. *Nature* **1997**, *386*, 377−379.
(3) Hynek, S.; Fuller, W.; Bentley, ? *Int. J. Hydrogen Energy* **1997**, *22*, 601−610.
(4) Ding, R. G.; Lu, G. Q.; Yan, Z. F.; Wilson, M. A. *J. Nanosci. Nanotechnol.* **2001**, *1*, 7−29.
(5) Dresselhaus, M. S.; Williams, K. A.; Eklund, P. C. *MRS Bull.* **1999**, 45−50.
(6) Schlapbach, L.; Züttel, A. *Nature* **2001**, *414*, 353−358.
(7) Cheng, H.-M.; Yang, Q.-H.; Liu, C. *Carbon* **2000**, *39*, 1447−1454.
(8) Li, J.; Furuta, T.; Goto, H.; Ohashi, T.; Fujiwara, Y.; Yip, S. *J. Chem. Phys.* **2003**, *119*, 2376−2385.
(9) Hirscher, M.; Becher, M. *J. Nanosci. Nanotechnol.* **2003**, *3*, 3−17.
(10) Wang, Q. Y.; Johnson, J. K. *J. Chem. Phys.* **1999**, *110*, 577−586.
(11) Darkrim, F.; Levesque, D. *J. Chem. Phys.* **1998**, *109*, 4981−4984.
(12) Rzepka, M.; Lamp, P.; de la Casa-Lillo, M. A. *J. Phys. Chem. B* **1998**, *110*, 10894−10898.
(13) Lee, S. M.; Lee, Y. H. *Appl. Phys. Lett.* **2000**, *76*, 2877−2879.
(14) Chan, S.-P.; Chen, G.; Gong, X. G.; Liu, Z.-F. *Phys. Rev. Lett.* **2001**, *87*, 205502.
(15) Lueking, A.; Yang, R. T. *J. Catal.* **2002**, *206*, 165−168.
(16) Shen, K.; Tierney, D. L.; Pietrass, T. *Phys. Rev. B* **2003**, *68*, 165418.
(17) Dillon, A. C.; Gennett, T.; Jones, K. M.; Alleman, J. L.; Parilla, P. A.; Heben, M. *J. Adv. Mater.* **1999**, *11*, 1354−1358.
(18) Chen, Y.; Chen, J.; Hu, H.; Hamon, M. A.; Itkis, M. E.; Haddon, R. C. *Chem. Phys. Lett.* **1999**, *299*, 532−535.
(19) Kuznetsova, A.; J. T. Yates, J.; Liu, J.; Smalley, R. E. *J. Chem. Phys.* **2000**, *112*, 9590−9598.
(20) Deutch, J. M.; Oppenheim, I. *Adv. Magn. Reson.* **1966**, *2*, 225−262.
(21) Raynes, W. T.; Davies, A. M.; Cook, D. B. *Mol. Phys.* **1971**, *21*, 123−133.
(22) Smith, M. R.; Bittner, E. W.; Shi, W.; Johnson, K. J.; Bockrath, B. C. *J. Phys. Chem. B* **2003**, *107*, 3752−3760.
(23) Schmid, M.; Krämer, S.; Goze, C.; Mehring, M.; Roth, S.; Bernier, P. *Synth. Met.* **2003**, *135−136*, 727−728.
(24) Jeener, J.; Meier, B. H.; Bachmann, P.; Ernst, R. R. *J. Chem. Phys.* **1979**, *71*, 4546−4553.

(25) Lipsicas, M.; Bloom, M. *Can. J. Phys.* **1961**, *39*, 881−907.
(26) Yu, I.; Lee, J.; Lee, S. G. *Physica B* **2003**, *329*−*333*, 421−422.
(27) Kleinhammes, A.; Mao, S.-H.; Yang, X.-J.; Tang, X.-P.; Shimoda, H.; Lu, J. P.; Zhou, O.; Wu, Y. *Phys. Rev. B* **2003**, *68*, 075418.
(28) Hou, P.-X.; Xu, S.-T.; Ying, Z.; Yang, Q.-H.; Liu, C.; Cheng, H.-M. *Carbon* **2003**, *41*, 2471−2476.
(29) Volpe, M.; Cleri, F. *Chem. Phys. Lett.* **2003**, *544*, 24−34.
(30) Shi, W.; Johnson, J. K. *Phys. Rev. Lett.* **2003**, *91*, 015504.
(31) Shen, K.; Pietrass, T. *Appl. Phys. Lett.* **2004**, *84*, 1567−1569.
(32) Shiraishi, M.; Ata, M. *J. Nanosci. Nanotechnol.* **2002**, *2*, 463−465.
(33) Narehood, D. G.; Kostov, M. K.; Eklund, P. C.; Cole, M. W.; Sokol, P. E. *Phys. Rev. B* **2002**, *65*, 233401.
(34) Fedorov, A. S.; Avramov, P. V.; Ovchinnikov, S. G.; Kresse, G. *Europhys. Lett.* **2003**, *63*, 254−260.